Diabetes, Metabolic Syndrome and Obesity: Targets and Therapy Dovepress
open access to scientific and medical research

Open Access Full Text Article

ORIGINAL RESEARCH

Mesenchymal Stem Cell-Derived Exosomes Carry MicroRNA-125a to Protect Against Diabetic Nephropathy by Targeting Histone Deacetylase 1 and Downregulating Endothelin-1

This article was published in the following Dove Press journal:
Diabetes, Metabolic Syndrome and Obesity: Targets and Therapy

Yan Hao[1]
Jie Miao[2]
Wenjia Liu[1]
Kangqin Cai[1]
Xianli Huang[1]
Li Peng[1]

[1]Department of Nephrology, The First People's Hospital of Zigong, Zigong, 643000, Sichuan, People's Republic of China; [2]Department of Nephrology, The Health and Rehabilitation Vocational College of Sichuan, Zigong, 643000, Sichuan, People's Republic of China

Background: Mesenchymal stem cell (MSC)-derived exosomes have seen great advances in human disease control in a minimally invasive manner. This research aimed to explore the function of MSC-derived exosomes in diabetic nephropathy (DN) progression and the molecules involved.

Methods: A rat model with DN and rat glomerular mesangial cell (GMC) models treated with high glucose (HG) were established, which were treated with exosomes from adipose-derived-MSCs (adMSCs). The levels of blood glucose, serum creatinine, and urinary protein, the urine albumin-to-creatinine ratio (UACR), kidney weight/body weight, and mesangial hyperplasia and kidney fibrosis in rats were determined. The expression of interleukin-6 (IL-6), collagen I (Col. I), fibronectin (FN), Bax and Bcl-2 in HG-treated GMCs was assessed. The microRNA (miRNA) carried by adMSC-exosomes was identified, and the implicated down-stream molecules were analyzed.

Results: adMSC-derived exosomes decreased levels of blood glucose, serum creatinine, 24-h urinary protein, UACR and kidney weight/body weight, and they suppressed mesangial hyperplasia and kidney fibrosis in DN rats. The exosomes also suppressed levels of IL6, Col. I and FN in HG-treated GMCs and promoted cell apoptosis. miR-125a was at least partially responsible for the above protective events mediated by adMSC-exosomes. miR-125a directly bound to histone deacetylase 1 (HDAC1), while HDAC1 further regulated endothelin-1 (ET-1) activation. Up-regulation of HDAC1 blocked the functions of adMSC-exosomal miR-125a.

Conclusion: This study suggested that adMSC-derived exosomes inhibit DN progression and alleviate the symptoms by carrying miR-125a, during which HDAC1 and ET-1 were inhibited. This study may provide novel effects into DN treatment.

Keywords: exosomes, miR-125a, HDAC1, ET-1, diabetic nephropathy

Introduction

Diabetic nephropathy (DN) is a disease characterized by stereotypical pathological structural and functional impairments in the kidneys of patients with diabetes mellitus (DM).[1] Although intensive administrations in controlling the glucose, lipids and blood pressure can retard the progression of DN, DN remains the most common cause of end-stage renal diseases.[2] Both genetic and environmental factors are involved in the DN pathogenesis that results in continuing and irreversible

Correspondence: Yan Hao
Department of Nephrology, The First People's Hospital of Zigong, No. 42, Shangyi Road, Daoshenghao Community, Ziliujing District, Zigong, 643000, Sichuan, People's Republic of China
Tel/Fax +86-13990087106
Email haoyan12301@163.com

submit your manuscript | www.dovepress.com
DovePress
http://doi.org/10.2147/DMSO.S286191

damage to the glomeruli and tubulointerstitial of the kidneys, contributing to renal function regression and the eventual renal failure.[3] The DM-induced renal dysfunction leads to high life-threatening morbidity, and heavy healthcare and financial burden across the globe. Identifying novel interventions to decrease the incidence or slow the disease progression is an urgent biomedical issue.

The ubiquitous mesenchymal stem cells (MSCs) in many tissues have been widely employed in clinical studies and accepted as an ideal candidate for cell-based therapies owing to their secretory capacity, mainly including the secreted extracellular vesicles (Evs).[4] Evs are small vesicles with common types including exosomes, microparticles and apoptotic bodies.[5] Exosomes are the most common Evs with a diameter from 30 to 120 nm that are abundant in numerous body fluids with the ability to mediate intercellular communication via carrying RNAs and proteins between cells or remote organs.[6] The therapeutic potential of MSCs is primarily thanks to their role in inflammation inhibition and tissue regeneration, and they are a major subject of research in kidney diseases including DN.[7] But the exact roles of MSC-derived exosomes in DN progression and the implicated molecules are too complex to be fully elucidated. In the present study, the exosomes from adipose-derived MSCs (adMSCs) were collected, and their roles in DN development were explored. Intriguingly, microRNA-125a (miR-125a) was found as a cargo of adMSC-derived exosomes, which was partially in line with a previous report.[8] miRNAs, the mostly investigated non-coding RNAs and a major type of cargo of exosomes or Evs, are well-known to play key functions of down-regulating mRNA expression and adjusting protein levels.[9] Here, our study identified histone deacetylase 1 (HDAC1) as a direct target of miR-125a. Although the direct roles of HDAC1 in DN, to the best of our knowledge, has not been mentioned before, it has been noted to participate in the pathogenesis of proteinuric kidney diseases.[10] Here, we hypothesized that adMSCs-derived exosomes exert protective functions in DN progression by carrying miR-125a and the following HDAC1 down-regulation. Both animal and cell models were constructed to validate this hypothesis and to explore the further potential molecules involved.

Materials and Methods

Cell Culture and Treatment

Adipose-derived mesenchymal stem cells (adMSCs, CP-R198) and rat glomerular mesangial cells (GMC, CP-R057) were purchased from Procell Life Science & Technology Co., Ltd. (Wuhan, Hubei, China). The cells were cultured in the adMSC-specific complete medium (CM-R198) or GMC-specific complete medium (CM-R057) in a 37°C incubator with constant humidity and 5% CO_2. The GMCs were subjected to high-glucose (HG) treatment (30 mM glucose treatment for 24 h) to mimic a DN condition in vitro. Cells treated with normal glucose (NG, 5.5 mM glucose) for 24 h were set as controls.

The sequence of HDAC1 was synthesized and subcloned to pcDNA3.1 vector (pcDNA-HDAC1, Invitrogen Inc., Carlsbad, CA, USA) by GenePharma Co., Ltd. (Shanghai, China). The endothelin-1 (ET-1)-specific small interfering RNA (siRNA-ET-1), miR-125a mimic/inhibitor and the corresponding negative control(NC) vectors including pcDNA3.1 empty vector, siRNA-NC and miRNA NC were designed and synthesized by GenePharma as well. All vectors/mimic were transfected into adMSCs or GMCs using the Lipofectamine 3000 Reagent (Invitrogen, Thermo Fisher Scientific Inc., Waltham, MA, USA).

Exosome Extraction and Purification

When the cell confluence reached 90%, the adMSCs were washed in phosphate-buffered saline (PBS) and cultured in serum-free medium (Yocon Biotechnology, Beijing, China) for 72 hours (h). Then, the medium was collected and centrifuged at 300 g at 4°C for 10 minutes (min), at 2,000g at 4°C for 20 min to discard the cell debris, and then at 10,000g at 4°C for 1 h to collect precipitates. The precipitates were further resuspended in serum-free DMEM containing 25 mM HEPES (pH = 7.4) and underwent a high-speed centrifugation again to discard supernatant. The precipitates were preserved at −80°C for further use.

Exosomes extracted from adMSCs without any transfection were named Exosomes, while those from adMSCs transfected with miR-125a mimic/inhibitor or NC were named Exo-mimic, Exo-inhibitor and Exo-NC, respectively. The exosomes were quantified using a bicinchoninic acid (BCA) kit (Thermo Fisher). In vitro, the HG-treated cells were treated with different concentrations of exosomes (1 μg, 2 μg, 3 μg, 4 μg and 5 μg) for 24 h, and the HG-treated cells further treated with PBS were set as controls. In vivo, 50 μg exosomes were administrated in rats through tail vein injection.[11,12]

Transmission Electron Microscopy (TEM)

The particle precipitates obtained after a high-speed centrifugation from 400 mL medium were fixed in 2%

glutaraldehyde at 4°C overnight. After PBS washes, the particle precipitates were fixed in 1% OsO_4 for 1 h, dehydrated in ethanol, and embedded in epoxy resin. Then, the embedded precipitates were cut into slices, which were further treated with saturated sodium periodate and 0.1 N hydrochloric acid for 10 min, and then observed under a TEM (JEM-1010, JEOL, Tokyo, Japan).

Nanoparticle Tracking Analysis (NTA)

The collected particles were diluted in PBS. The particle size was analyzed using a NanoSight NTA Kit (Malvern Panalytical, UK) as per the manufacturer's protocols. Three independent experiments were performed.

Western Blot Analysis

Total protein was collected using Radio-Immunoprecipitation assay cell lysis buffer, and the protein concentration was determined using the BCA kit. The protein was then separated by 6% SDS-PAGE and transferred onto polyvinylidene fluoride membranes. The membranes were blocked with 5% non-fat milk at 20°C for 1 h and incubated with the primary antibodies prepared in 5% bovine serum albumin at 4°C overnight, followed by incubation with the secondary antibodies in 5% non-fat milk at 20°C for 1.5 h. After that, the membranes were soaked in enhanced chemiluminescence reagent (WBKLS0100, Millipore, Corp. Billerica, MA, USA) and then exposed for film development. The protein bands with immunoblots were analyzed, and the relative protein level was calculated based on the gray value ratio of target bands and internal references. Three independent experiments were performed. The antibodies used were TSG101 (1:2000, ab125011, Abcam, Cambridge, UK), CD9 (1:2000, ab92726, Abcam), CD63 (1:100, ab108950, Abcam), Bax (1:5000, ab32503, Abcam), Bcl-2 (1:2000, ab196495, Abcam), β-actin (1:11,000, ab6276, Abcam) and HDAC1 (1:2000, ab7028, Abcam) and HRP-labeled secondary antibodies goat anti-rabbit IgG (1:50,000, ab205718, Abcam) and goat anti-mouse IgG (1:10,000, ab205719, Abcam).

Reverse Transcription Quantitative Polymerase Chain Reaction (RT-qPCR)

TRIzol reagent (Invitrogen, USA) was used to collect total RNA from cells and tissues. The RNA was reversely transcribed into cDNA using a SuperScriptRT Kit (Invitrogen, USA). Then, the cDNA was collected for real-time qPCR using the SYBR Green Master Mix (Applied Biosystems Inc., Carlsbad, CA, USA) on an ABI PRISM 7300 RT-PCR System (Applied Biosystems). The primer sequences are listed in Table 1, and the relative RNA expression was determined using the $2^{-\Delta\Delta Ct}$ method with U6 and GAPDH as the internal references for miRNA and mRNAs, respectively.

Table 1 Primer Sequences in RT-qPCR

Gene	Primer Sequence (5′-3′)
miR-125a	F: TCCCTGAGACCCTTTAACCT R: GAACATGTCTGCGTATCTC
HDAC1	F: TGAAGCCTCACCGAATCCGCAT R: TGGTCATCTCCTCAGCATTGGC
ET-1	F: CTACTTCTGCCACCTGGACATC R: CGCACTGACATCTAACTGCCTG
Col. I	F: CCTCAGGGTATTGCTGGACAAC R: CAGAAGGACCTTGTTTGCCAGG
FN	F: CCCTATCTCTGATACCGTTGTCC R: TGCCGCAACTACTGTGATTCGG
IL-6	F: TACCACTTCACAAGTCGGAGGC R: CTGCAAGTGCATCATCGTTGTTC
GAPDH	F: GCACCGTCAAGGCTGAGAAC R: TGGTGAAGACGCCAGTGGA
U6	F: GCTTCGGCAGCACATATACTAAAA R: GCTTCGGCAGCACATATACTAAAAT

Abbreviations: RT-qPCR, reverse transcription quantitative polymerase chain reaction; HDAC1, histone deacetylase 1; ET-1, endothelin-1; Col. I, collagen I; FN, fibronectin; IL-6, interleukin-6; GAPDH, glyceraldehyde-3-phosphate dehydrogenase.

Animal Experiment

Male Sprague-Dawley rats (6 weeks old, 200 ± 20 g) were purchased from Vital River Laboratory Animal Technology Co., Ltd. (Beijing, China). The rats were housed in a standard animal room in a 12-h dark/light cycle with free access to feed and water. Animal experiments were ratified by the Animal Care and Use Committee of the First People's Hospital of Zigong. All experimental procedures were conducted in strict accordance with the Guide for the Care and Use of Laboratory Animals issued by National Institutes of health (NIH, Bethesda, Maryland, USA). Great attempts were made to minimize the usage and suffering of animals.

After one week of acclimation, a rat model with DN was established as previously reported.[13] The animals were starved overnight, and then injected with 60 mg/kg streptozotocin (STZ, Sigma-Aldrich Chemical Company,

St Louis, MO, USA, dissolved in 0.1 M citric acid buffer) through intraperitoneal injection. Rats in the control group were given an equal volume of citric acid buffer alone (n = 10). Rats with a blood glucose level over 16.7 mmol/L for continuous three days were considered as successfully established DN models. From the 4th week to 6th week after STZ injection, the urine samples of rats were collected and the concentration of urinary protein was determined. An over 30-mg urinary protein level within 24 h was considered a successful establishment of DN model.[14] The model rats required for further experiments were obtained through repeated experiments.

On the 7th week after STZ injection, the DN rats were allocated into 8 groups, 10 in each: DN group (model rats); PBS group (model rats were injected with 200 μL PBS through caudal vein twice a week for 3 weeks); Exosomes group (model rats were injected with 50 μg exosomes through caudal veins twice a week for 3 weeks); Exo-NC group (model rats were injected with 50 μg Exo-NC through caudal veins twice a week for 3 weeks); Exo-mimic group (model rats were injected with 50 μg Exo-mimic through caudal veins twice a week for 3 weeks); Exo-inhibitor group (model rats were injected with 50 μg Exo-inhibitor through caudal veins twice a week for 3 weeks); Exo-mimic + LV-NC (on the basis of treatments in the Exo-mimic group, the mice were further injected with LV-NC from the second week after the first-time Exo-mimic transfection through caudal veins for two times); and Exo-mimic + LV-HDAC1 (on the basis of treatments in the Exo-mimic group, the mice were further injected with LV-HDAC1 from the second week after the first-time Exo-mimic transfection through caudal veins for two times).

The exosomes for transfection were dissolved in 200 μL PBS, and the rats in the PBS (control) group were injected with an equal volume of PBS. The LV-NC and LV-HDAC1 were acquired from GenePharma. The virus titer was 1×10^9 TU/mL, and the injection volume was 10 μL each time. The blood and urine samples of each group of rats were collected and preserved at −80°C for further use. After that, the rats were euthanized by overdose of pentobarbital sodium (200 mg/kg), and then the blood and kidney tissue samples were collected for further analysis.

Biochemical Test

The collected blood samples were centrifuged at 5000 g at 4°C for 10 min. Then, the serum was collected, and the level of blood glucose was determined using a Glucose LiquiColor® Test (Stanbio Laboratory, Boerne, TX, USA), while the serum creatinine level was determined using an automatic biochemical analyzer (AU5800, Beckman Coulter Inc., Brea, CA, USA).

Rats were kept separately in metabolic cages to have the urine samples collected. The 24-h urinary protein level was evaluated using an enzyme-linked immunosorbent assay (ELISA) kit (JianglaiBio, Shanghai, China) according to the kit's instructions. In addition, the urine creatinine level was examined using an automatic biochemical instrument, and the urinary microalbumin was examined using a rat microalbuminuria (MAU/ALB) ELSA kit (CSB-E12991r, USCN kit Inc., Hubei, China). Then, the urinary albumin creatinine ratio (UACR) was calculated.

Histological Examination of Kidney

The cortex of the right kidneys of rats was dissected and at −80°C for RNA protein extraction. The remaining kidney tissues were fixed in 4% paraformaldehyde, embedded in paraffin, and cut into 4-μm sections. Then, the sections were stained with a Periodic Acid-Schiff (PAS) staining kit (Sbjbio Life Sciences, Nanjing, Jiangsu, China) and observed under an optical microscope (magnification × 400). The proportion of PAS staining area to total area of the glomerulus was examined using the Image J software (NIH). In each group of kidney tissues, 20 glomeruli were collected. In addition, hematoxylin and eosin (HE) staining was conducted to examine the pathological changes in rat kidney tissues. The staining in 20 random glomerular areas was scored by three pathologists who had no idea of the grouping details, and the scoring was performed according to tubular cell necrosis, cytoplasmic vacuole formation, hemorrhage, and tubular dilatation.[15] Moreover, immunohistochemical staining was performed to examine the protein level of a fibrosis-marker collagen I (Col. I) in the rat kidney tissues using anti-collagen I (1:200, ab254113, Abcam). To each tissue section, 20 continuous fields of views were observed and the integrated optical density (IOD) value was examined using the Image J to examine the expression of Col. I.

RNA Immunoprecipitation (RIP) Assay

The enrichment of ET-1 by HDAC1 protein was examined using a Magna RIP™ RNA-binding Protein Immunoprecipitation Kit (Millipore) according to the kit's instructions. In short, the GMCs were crosslinked in 0.3% methanol and then quenched using glycine solution. The magnet beads were incubated with anti-HDAC1

(Abcam) or anti-IgG (Millipore, Massachusetts, USA) at 25°C for 30 min. Then, the cell lysates were incubated with the treated magnet beads at 4°C overnight. After that, the RNA-protein compounds were detached in proteinase K buffer at 55°C for 45 min. The enriched RNA was extracted using phenol:chloroform:isopentanol (125:24:1). The purified RNA was examined using RT-qPCR to detect the abundancy of ET-1.

Dual-Luciferase Reporter Gene Assay

The wild-type (WT) HDAC1 3′UTR fragment containing the putative binding site with miR-125a was sub-cloned to the pmiRGLO vector (Promega, Madison, WI, USA) and named HDAC1-3′UTR-WT. The vector constructed with the mutant type (MT) of HDAC1 sequence was named HDAC1-3′UTR-MT. The constructed recombined vectors were co-transfected with miR-125a mimic/inhibitor or the mimic/inhibitor control into GMCs. Cells were collected 24 h later and incubated with passive cell lysis buffer at room temperature for 10 min. Then, the relative luciferase activity was determined using a Dual-Luciferase Reporter Kit (Promega) as per the manufacturer's instructions.

Cell Counting Kit-8 (CCK-8) Assay

A CCK-8 kit (Dojindi Molecular Technologies, Gaithersburg, Maryland, USA) was used to examine the proliferation ability of cells at different time points. In short, GMCs were seeded onto 96-well plates at 5×10^4 cells/mL and incubated at 37°C with 5% CO_2. Each well was loaded with CCK-8 Reagent at different time points (12 h, 24 h, 48 h, 72 h), followed by another 2 h of incubation at 37°C. Then, the optical density at 450 nm was detected. Viability of cells after different doses of exosome treatment was examined as well. The HG-treated GMCs (1×10^4 cells per well) were treated with exosomes at different concentrations (1 μg, 2 μg, 3 μg, 4 μg and 5 μg) for 24 h, and cells treated with PBS were set as control. After that, the GMCs were treated with 10 μL CCK-8 solution for 2 h, and then the optical density was examined.

Statistical Analysis

Data were analyzed using SPSS 22.0 (IBM Corp. Armonk, NY, USA). Data were exhibited as mean ± standard error of mean (SEM) from no less than three independent experiments. Differences were compared utilizing the *t* test (two groups) and one-way or two-way analysis of variance (ANOVA) (multiple groups) followed by Tukey's multiple comparison test. The *p* value was obtained from two-tailed tests with $p < 0.05$ regarded as statistically significant. Each experiment was performed in triplicate with the average value calculated.

Results

adMSC-Derived Exosomes Reduce DN Symptoms in Model Rats

The key functions of MSC-derived exosomes have been documented in multiple human diseases. Here, the exosomes from adMSCs were collected. The collected particles presented typical circular shape under the TEM (Figure 1A). The NTA results showed that the diameter of the particles was about 30–120 nm (Figure 1B). In addition, the Western blot analysis confirmed positive expression of exosome-specific biomarkers TSG101, CD9 and CD63 (Figure 1C) in the particles. These findings collectively identified that the collected particles from adMSC were exosomes.

Aberrant levels of blood glucose, serum creatinine, and urinary protein are closely linked to DN progression. We therefore determined the change in blood glucose level, as well as the levels of serum creatinine, urinary protein, UACR and kidney weight/body weight in rats 9 weeks after model establishment. The DN rats showed a significant increase in blood glucose, serum creatinine, urinary protein levels and UACR compared to the control ones, and the kidney weight of the DN model rats was increased as well. Importantly, injection of exosomes led to a decline in these levels in rats compared to PBS injection (Figure 1D). Aberrant proliferation of GMCs leads to mesangial matrix expansion, which represents a major characteristic of DN.[16] We therefore observed the expansion of mesangial matrix in rat kidneys by PAS staining (Figure 1E). It was found that the expansion rate of mesangial matrix in DN rats was significantly increased. PBS treatment showed little impact on the symptoms, while injection of exosomes reduced the expansion in rats. In addition, HE staining was further performed to determine the pathological changes in rat kidney tissues (Figure 1F). Compared to rats in the control group, rats in the DN group showed significant pathological symptoms including capillary lumen shrinking, inflammatory cell infiltration and renal tubular injury. Compared to PBS treatment, the exosomes significantly alleviated the kidney damage in the DN rats. Moreover, IHC staining was performed to examine the level of Col. I in rat kidney

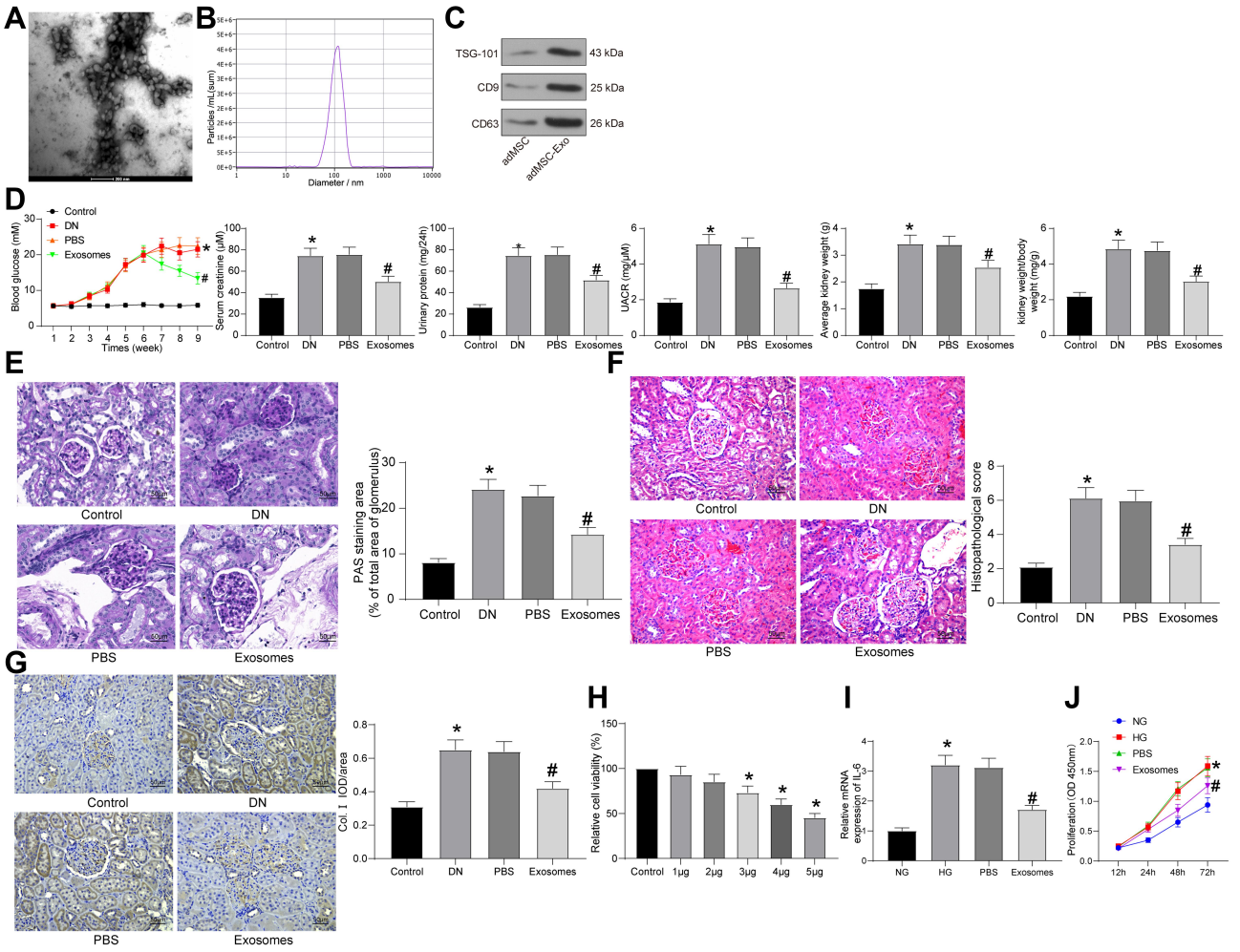

Figure 1 adMSC-derived exosomes reduce DN symptoms in model rats. (**A**) Round nanoparticles observed under the TEM; (**B**) diameter of the collected particles measured by NTA; (**C**) levels of exosome-specific surface biomarkers TSG101, CD9 and CD63 determined by Western blot analysis; (**D**) changes in physiological parameters in each group of rats (one-way ANOVA, $^{*}p < 0.05$ vs Control; $^{\#}p < 0.05$ vs PBS); (**E**) mesangial hyperplasia in rat kidney tissues determined by PAS staining (one-way ANOVA, $^{*}p < 0.05$ vs Control; $^{\#}p < 0.05$ vs PBS); (**F**) pathological changes in rat kidneys examined by HE staining (one-way ANOVA, $^{*}p < 0.01$ vs Control; $^{\#}p < 0.05$ vs PBS), (**G**) protein level of the fibrosis-related marker Col. I in rat kidney determined by IHC staining (one-way ANOVA, $^{*}p < 0.05$ vs Control; $^{\#}p < 0.05$ vs PBS); (**H**) viability of GMCs after different concentrations of exosomes (1 μg, 2 μg, 3 μg, 4 μg and 5 μg) or PBS treatment determined by the CCK-8 method (one-way ANOVA, $^{*}p < 0.05$ vs Control); (**I**) IL-6 mRNA expression in GMCs determined by RT-qPCR (one-way ANOVA, $^{*}p < 0.01$ vs NG; $^{\#}p < 0.05$ vs PBS); (**J**) proliferation ability of GMCs determined using the CCK-8 method (one-way ANOVA, $^{*}p < 0.01$ vs NG; $^{\#}p < 0.05$ vs PBS). N = 10 in each group. Data were exhibited as mean ± SEM from three independent experiments. Representative images are provided.

(Figure 1G). It was noteworthy that the protein expression of Col. I was increased in the kidney of DN rats. PBS treatment did not affect the expression of Col. I, while the exosomes significantly blocked the upregulation of Col. I in rats.

Following the findings above, we further explored the functions of the adMSC-exosomes in vitro. GMCs were treated with HG to mimic a DN-like condition in vitro, which were further treated with different concentrations of exosomes (1 μg, 2 μg, 3 μg, 4 μg and 5 μg) or PBS. Viability of cells 24 h of exosome or PBS treatment was examined using the CCK-8 method (Figure 1H). It was found that the viability of GMCs was significantly enhanced by HG, but further treatment of exosomes reduced the cell viability in a dose-dependent manner. Treatment of 5 μg exosomes reduced viability of the HG-treated GMCs by half. Therefore, this dose was selected for the subsequent experiments.

IL-6 is a typical autocrine growth factor for rat GMCs which promotes mesangial hyperplasia.[17] Therefore, we determined IL-6 expression in each group of cells using RT-qPCR. It was found that HG treatment significantly enhanced IL-6 expression in GMCs, while the IL-6 expression was significantly reduced after exosome treatment but not PBS (Figure 1I). The CCK-8 assay suggested that the proliferation ability of GMCs was increased after

HG treatment, while the proliferation of cells was suppressed as well after exosome treatment (Figure 1J). These results preliminarily identified the protective roles of adMSC-derived exosomes in DN.

adMSC-Derived Exosomes Exert Functions by Carrying miR-125a

A previous study suggested that miR-125a is enriched in MSC-derived exosomes,[8] and this miRNA has been noted to be poorly expressed in DN patients.[18] Then, we inferred that adMSC may carry miR-125a to protect DN.

Subsequently, we transfected miR-125a mimic/inhibitor and the corresponding NC vector into adMSCs, and the exosomes from adMSC after different treatments were collected and termed Exo-mimic, Exo-inhibitor and Exo-NC, respectively. Next, the RT-qPCR identified the highest expression of miR-125a in the Exo-mimic, while the lowest expression of miR-125a was found in Exo-inhibitor, and the miR-125a showed no notable differences between normal Exosomes and Exo-NC (Figure 2A). Therefore, we confirmed the abundant existence of miR-125a in the adMSC-derived exosomes.

To further explore the roles of exosomal miR-125a in DN, the different exosomes were injected into DN rats with PBS injection as control. Also, the control rats were included for comparison. The change in blood glucose level, and the levels of serum creatinine, urinary protein, UACR and kidney weight/body weight in rats after 9 weeks were examined. Compared to control rats, the PBS-treated DN model rats showed significant physiological changes such as rises in blood glucose, serum creatinine, 24-h urinary protein, UACR and increased kidney weight. However, compared to PBS injection, Exo-NC suppressed the levels of blood glucose, serum creatinine, 24-h urinary protein, as well as UACR and kidney weight in DN rats. It was noteworthy that the alleviating effects of Exo-NC on kidney symptoms were strengthened by Exo-mimic but blocked by Exo-inhibitor (Figure 2B). In addition, the PAS staining results suggested that the mesangial hyperplasia was significantly increased in the PBS-treated DN rats compared to the control rats. Compared to PBS treatment, the Exo-NC inhibited mesangial hyperplasia in DN rats. This inhibition was strengthened by Exo-mimic while blocked by Exo-inhibitor (Figure 2C). The HE staining results (Figure 2D) showed that PBS treatment did not alleviate the pathological symptoms in DN rats. Importantly, Exo-NC relieved the symptoms in rats, and the protective functions of further enhanced upon miR-125a upregulation but blocked after miR-125a inhibition. In addition, the IHC staining results (Figure 2E) showed that Exo-NC reduced the protein level of Col. I in rat kidney compared to PBS treatment. Again, this reduction was strengthened by Exo-mimic but reduced by Exo-inhibitor

As for in vitro experiments, these exosomes and PBS were transfected into the HG-treated GMCs, and the GMCs treated with NG were set as control. Then, the expression of apoptosis-related factors Bcl-2 and Bax in cells was determined. Compared to control cells, the expression of anti-apoptotic Bcl-2 was increased while the expression of pro-apoptotic Bax was reduced in the PBS/HG-treated GMCs. Importantly, Exo-NC treatment increased the expression of Bax while reduced the expression of Bcl-2 in the HG-treated cells. These changes were even more notable in cells treated with Exo-mimic but less notable in cells treated with Exo-inhibitor (Figure 2F). In addition, fibrosis of GMCs is another major driver of the DN progression.[19] Then, RT-qPCR was performed to examine the mRNA expression of fibrosis-related factors Col. I and fibronectin (FN) in cells. It was found that the expression of Col. I and FN was increased in HG-treated GMCs. Compared to PBS treatment, Exo-NC led to reduced mRNA expression of Col. I and FN in the GMCs. This reduction was more profound in cells treated with Exo-mimic but less notably in cells treated with Exo-inhibitor (Figure 2G). These results confirmed that the miR-125a was responsible for the kidney protective events by adMSC-derived exosomes.

miR-125a Directly Binds to HDAC1

We next explored the downstream molecules involved. First, an online prediction on miRwalk (http://mirwalk.umm.uni-heidelberg.de/) suggested miR-125a has binding sites with rno-HDAC1 (Figure 3A). HDAC1 has been documented to be highly expressed in DN.[20] To further validate the binding relationship between miR-125a and HDAC1, we determined HDAC1 expression in the kidney tissues in rats and in GMCs. The RT-qPCR and Western blot results showed that HDAC1 was highly expressed in DN rats as well as in HG-treated GMCs (Figure 3B). In addition, miR-125a mimic/inhibitor and the corresponding NC vector were administrated into HG-treated GMCs, and it was found the HDAC1 expression was notably inhibited by miR-125a mimic (Figure 3C). Moreover, a dual-luciferase reporter gene assay was performed, which found the luciferase

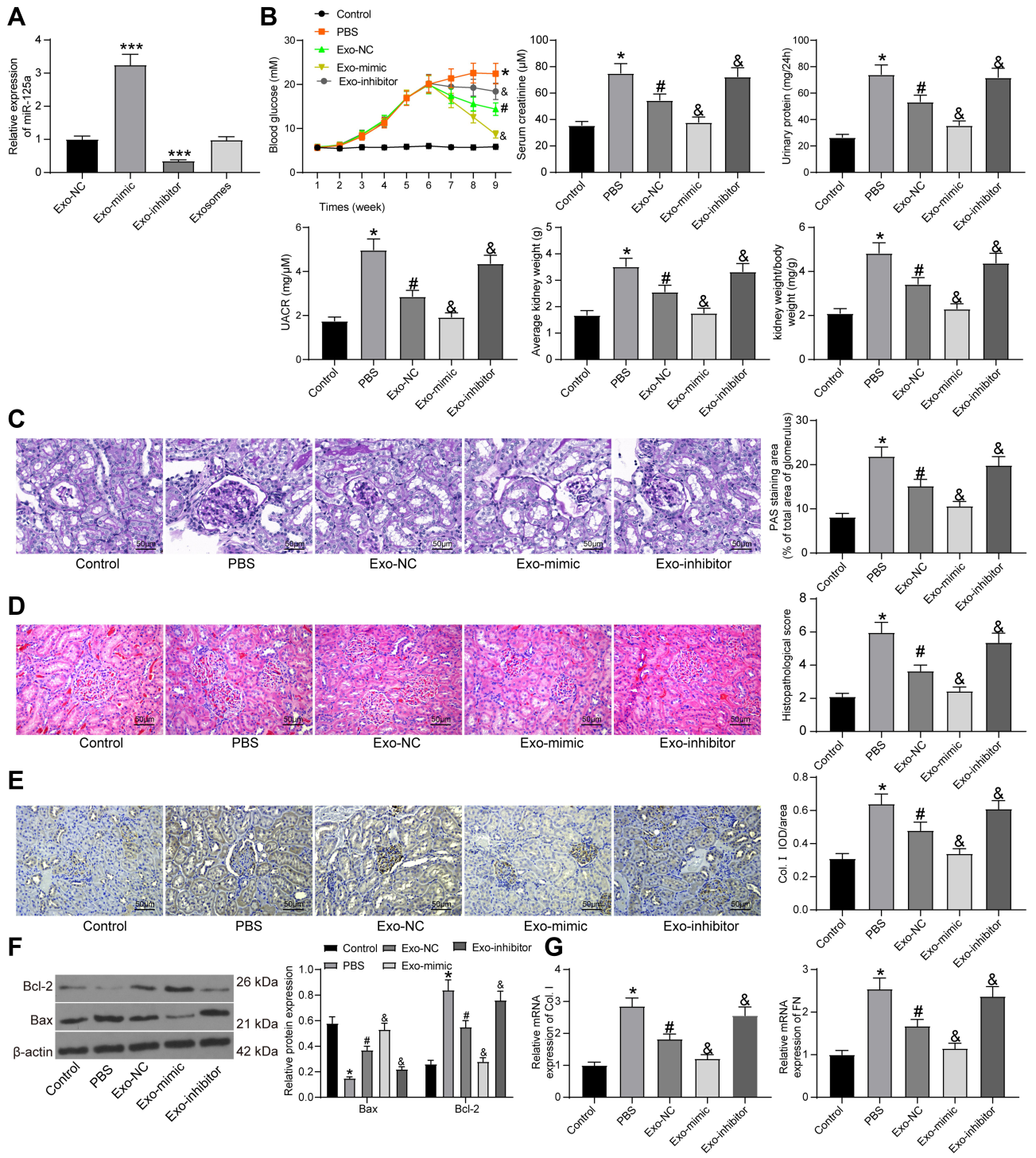

Figure 2 adMSC-derived exosomes exert functions by carrying miR-125a. (**A**) miR-125a expression in each group of exosomes determined by RT-qPCR (one-way ANOVA, compared to Exo-NC, ***$p < 0.001$); (**B**) changes in physiological parameters in each group of rats (one-way ANOVA, *$p < 0.05$ vs Control, $^{\#}p < 0.05$ vs PBS, $^{\&}p < 0.05$ vs Exo-NC); (**C**) mesangial hyperplasia in rat kidney tissues determined by PAS staining (one-way ANOVA, *$p < 0.05$ vs Control, $^{\#}p < 0.05$ vs PBS, $^{\&}p < 0.05$ vs Exo-NC); (**D**) pathological changes in rat kidneys examined by HE staining (one-way ANOVA, *$p < 0.05$ vs Control, $^{\#}p < 0.05$ vs PBS, $^{\&}p < 0.05$ vs Exo-NC), (**E**) protein level of the fibrosis-related marker Col. I in rat kidney determined by IHC staining (one-way ANOVA, *$p < 0.05$ vs Control, $^{\#}p < 0.05$ vs PBS, $^{\&}p < 0.05$ vs Exo-NC); (**F**) protein levels of Bax and Bcl-2 in rat kidney tissues determined by Western blot analysis (one-way ANOVA, *$p < 0.05$ vs Control, $^{\#}p < 0.05$ vs PBS, $^{\&}p < 0.05$ vs Exo-NC); (**G**) mRNA expression of Col. I and FN in HG-treated GMC cells determined by RT-qPCR (one-way ANOVA, *$p < 0.05$ vs Control, $^{\#}p < 0.05$ vs PBS, $^{\&}p < 0.05$ vs Exo-NC). N = 10 in each group. Data were exhibited as mean ± SEM from three independent experiments. Representative images are provided.

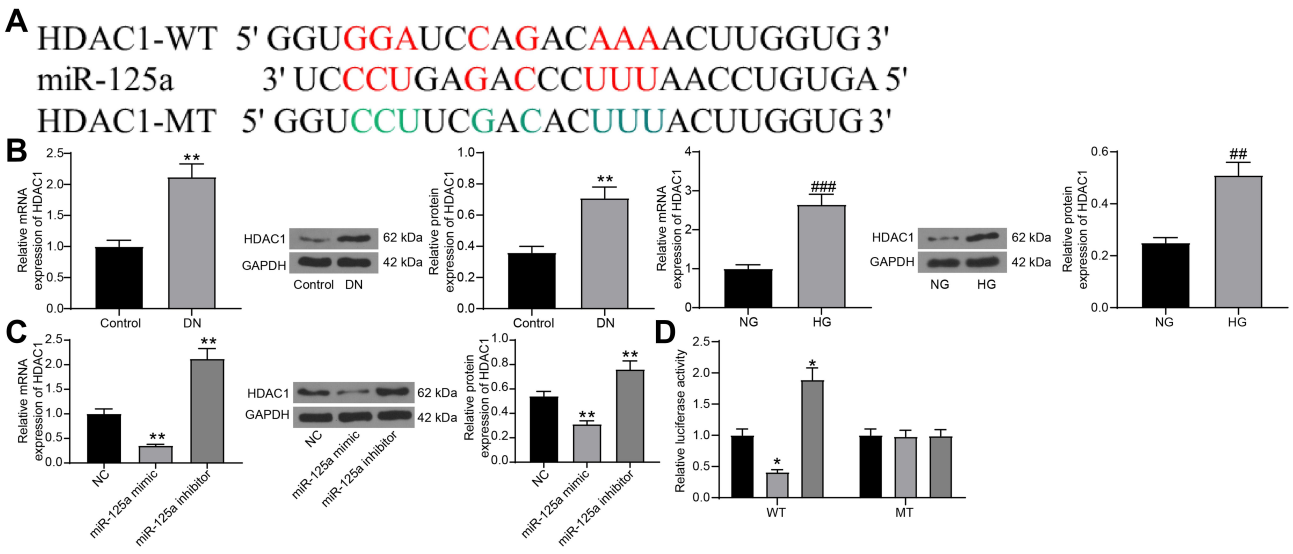

Figure 3 miR-125a directly binds to HDAC1. (**A**) putative binding sequence of miR-125a and HDAC1 predicted on miRwalk; (**B**) RT-qPCR and protein expression of HDAC1 in kidney tissues in DN rats and in GMCs determined by RT-qPCR and Western blot analysis (unpaired *t* test, $^{**}p < 0.01$ vs Control; $^{\#\#}p<0.01, ^{\#\#\#}p < 0.001$ vs NG); (**C**) HDAC1 expression in HG-treated SV40-MES1 cells post miR-125a mimic/inhibitor/NC transfection determined using RT-qPCR and Western blot analysis (one-way ANOVA, $^{**}p < 0.01$ vs NC); (**D**) binding relationship between miR-125a and HDAC1 validated by a dual-luciferase reporter gene assay (one-way ANOVA, $^{*}p < 0.05$ vs NC). N = 10 in each group. Data were exhibited as mean ± SEM from three independent experiments.

activity of WT-HDAC1 was decreased when co-transfected with miR-125a mimic, while the activity was increased when co-transfected with miR-125a inhibitor, and neither the mimic nor inhibitor presented no differences in luciferase activity of MT-HDAC1 (Figure 3D). These findings collectively identified that miR-125a directly binds to HDAC1.

HDAC1 Interacts with ET-1 in DN

Interestingly, HDAC1 has been reported to interact with ET-1,[21] which has been suggested as a potential target of DN treatment.[22] But if HDAC1 regulates ET-1 in DN requires experimental evidence. Here, our study found high expression of ET-1 both in DN model rats and in HG-treated GMCs using RT-qPCR (Figure 4A). In addition, the RIP assay suggested that the ET-1 mRNA was enriched by the HDAC1 protein (Figure 4B).

HDAC1 Regulates ET-1 to Promote DN Progression

Following the findings above, we transferred pcDNA-HDAC1 into the HG-treated GMCs, after which the HDAC1 expression was successfully increased (Figure 5A). Then, HG-treated GMCs were, respectively, transfected with pcDNA, pcDNA-HDAC1, pcDNA-HDAC1 + siRNA-NC, pcDNA-HDAC1 + siRNA-ET-1, after which we found that pcDNA-HDAC1 led to a significant increase in ET-1 expression while siRNA-ET1 suppressed HDAC1

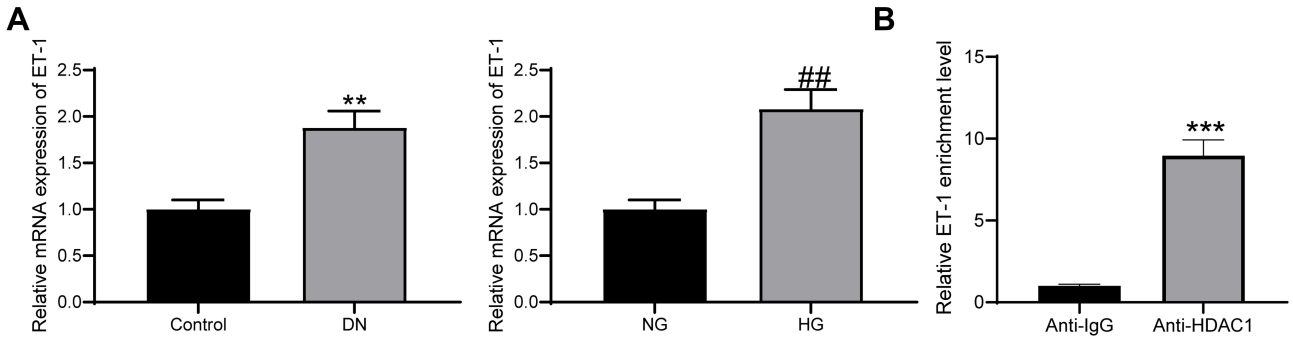

Figure 4 HDAC1 interacts with ET-1. (**A**) ET-1 was highly expressed in DN rats and HG-treated GMCs (unpaired *t* test, $^{**}p < 0.01$ vs Control; $^{\#\#}p < 0.01$ vs NG); (**B**) enrichment of ET-1 mRNA fragments in the compound pulled down by anti-HDAC1 or anti-IgG (unpaired *t* test, $^{***}p < 0.001$). N = 10 in each group. Data were exhibited as mean ± SEM from three independent experiments.

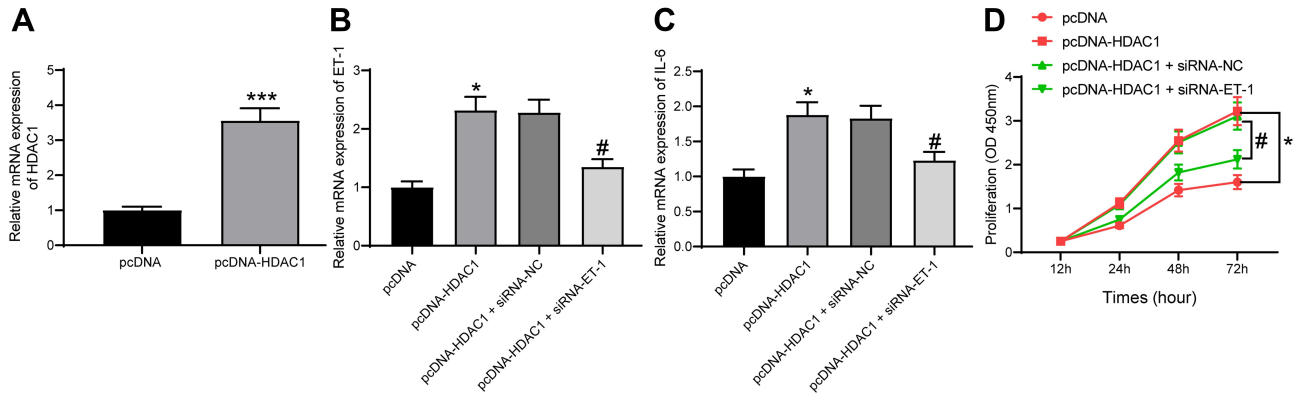

Figure 5 HDAC1 regulates ET-1 to promote DN progression. (**A**) HDAC1 expression in HG-treated GMCs after pcDNA-HDAC1 transfection determined by RT-qPCR (unpaired *t* test, ***$p < 0.001$); (**B**) ET-1 expression in each group of GMCs determined by RT-qPCR (one-way ANOVA, *$p < 0.05$ vs pcDNA; #$p < 0.05$ vs pcDNA-HDAC1 + siRNA-NC); (**C**) IL-6 expression in each group of GMCs determined by RT-qPCR (one-way ANOVA, *$p < 0.05$ vs pcDNA; #$p < 0.05$ vs pcDNA-HDAC1 + siRNA-NC); (**D**) proliferation of each group of cells determined by CCK-8 method (two-way ANOVA, *$p < 0.05$ vs pcDNA; #$p < 0.05$ vs pcDNA-HDAC1 + siRNA-NC). Data were exhibited as mean ± SEM from three independent experiments.

expression (Figure 5B). Then, RT-qPCR found that IL-6 secretion in cells was increased by pcDNA-HDAC1 but inhibited by siRNA-ET-1 (Figure 5C). Proliferation of glomerular mesangial cells is an important marker in DN pathogenesis. Here, we found that the proliferation of HG-treated GMCs was increased by pcDNA-HDAC1 but decreased by siRNA-ET-1 (Figure 5D). These results suggested that HDAC1 could aggravate DN progression by mediating ET-1.

adMSC-Derived Exosomal miR-125a Protects DN in Rats Through Inhibiting the HDAC1/ET1 Axis

In the subsequent experiments, we transferred the HDAC1-overexpressing vector LV-HDAC1 into DN rats after Exo-mimic injection, and then the levels of blood glucose, serum creatinine, and urinary protein in rats were determined. It was found that the suppressive function of Exo-mimic on the levels of blood glucose, serum creatinine, 24-h urinary protein, UACR and rat kidney tissues was blocked by LV-HDAC1 (Figure 6A). Then, the RT-qPCR results suggested that the expression of HDAC1 and ET1 in rat kidney tissues was notably increased (Figure 6B). Likewise, the inhibitory effect of Exo-mimic on mesangial hyperplasia in rat kidney was blocked after HDAC1 overexpression as well (Figure 6C). The HE staining results showed that the protective function of Exo-mimic against pathological symptoms in rats was blocked upon HDAC1 upregulation (Figure 6D). The IHC staining results also suggested that overexpression of HDAC1 increased the expression of Col. I in rat kidney (Figure 6E). Similar trends were found in vitro where the Exo-mimic-treated GMCs were transfected with pcDNA-HDAC1. The RT-qPCR results showed that the expression of HDAC1 and ET-1 in the GMCs was increased after pcDNA-HDAC1 treatment, and the expression of fibrosis-biomarkers Col. I and FN in cells was increased as well (Figure 6F). Moreover, the Western blot analysis results showed that pcDNA-HDAC1 led to increased expression of Bax while reduced expression of Bcl-2 (Figure 6G). Namely, the anti-apoptotic role of Exo-mimic in HG-treated GMCs was blocked by HDAC1.

Discussion

The current traditional therapeutic drugs for DN mainly include antihypertensive and antiproteinuric measures working by renin-angiotensin-aldosterone system inactivation; however, they are suboptimal with limited curative effect and there is an unmet need for therapies that provide effective regimens beyond glucose control.[23] Here, the study identified that adMSM-derived exosomes hold the potential to alleviate DN pathogenesis.

The initial finding of the study was that the exosomes extracted from adMSCs notably levels of blood glucose, serum creatinine, urinary protein, UACR, and suppressed mesangial hyperplasia and kidney fibrosis in STZ-induced DN rat models. Also, the exosomes decreased the concentration of IL-6, a typical autocrine growth factor for rat GMCs that promotes mesangial hyperplasia,[17] and reduced the fibrosis-related factors Col. I and FN in HG-treated GMCs. Increased Col. I and FN are key biomarkers for extracellular matrix expansion, contributing to renal fibrosis and impaired renal function.[24] Continuing fibrosis and

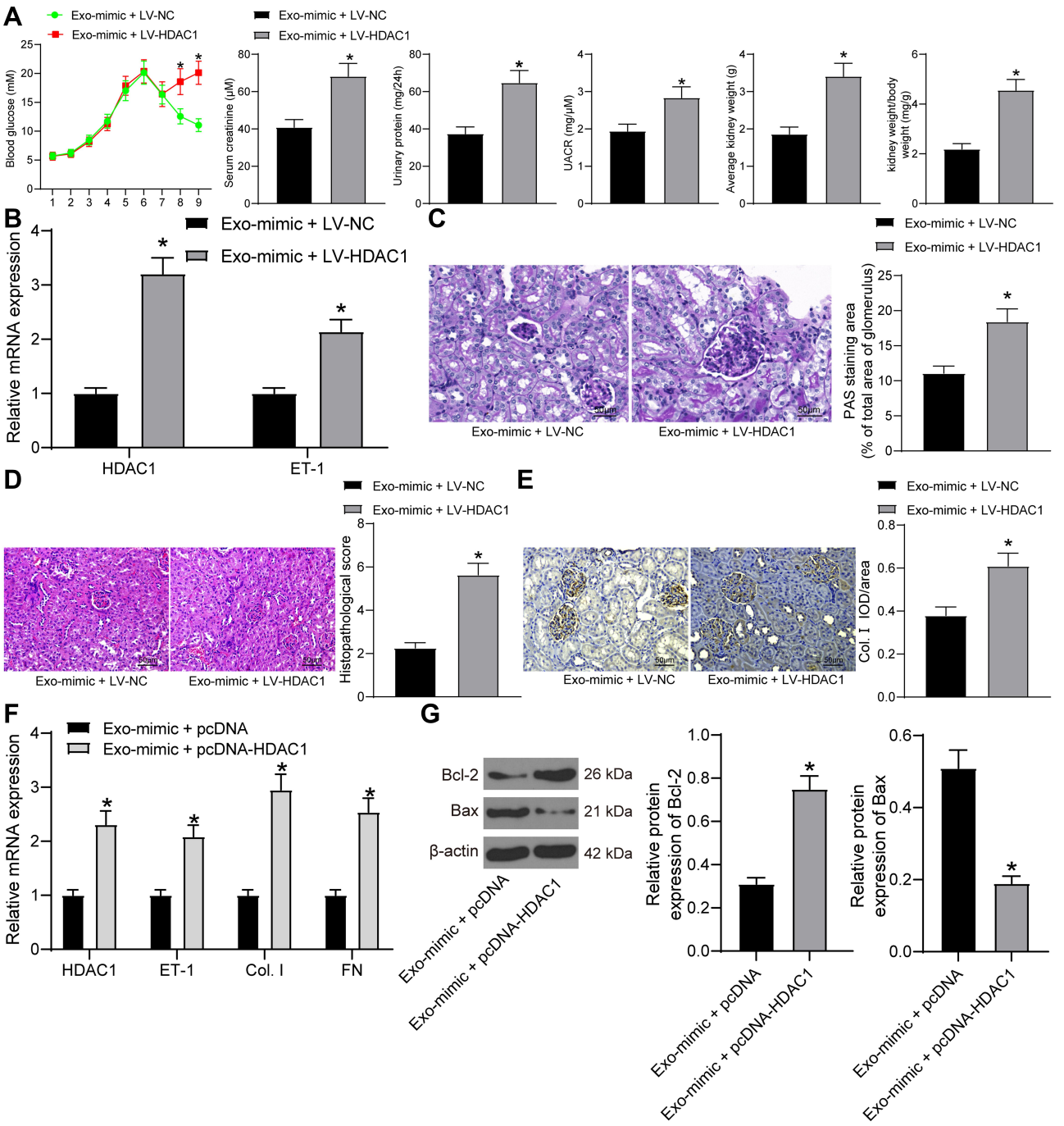

Figure 6 adMSC-derived exosomal miR-125a protects DN through inhibiting the HDAC1/ET1 axis. (**A**) levels of blood glucose, serum creatinine and 24-h urinary protein in each group of rats (unpaired *t* test, **p* < 0.05); (**B**) expression of HDAC1 and ET-1 in the kidney tissues of rats determined by RT-qPCR (two-way ANOVA, **p* < 0.05 vs Exo-mimic + LV-NC); (**C**) mesangial hyperplasia in rat kidney tissues determined by PAS staining (unpaired *t* test, **p* < 0.05); (**D**) changes in physiological parameters in each group of rats (unpaired *t* test, **p* < 0.05); pathological changes in rat kidneys examined by HE staining (unpaired *t* test, **p* < 0.05), (**E**) protein level of the fibrosis-related marker Col. I in rat kidney determined by IHC staining (unpaired *t* test, **p* < 0.05); (**F**) mRNA expression of HDAC1, ET-1, Col. I and FN in cells determined by RT-qPCR (two-way ANOVA, **p* < 0.05 vs Exo-mimic + LV-NC); (**G**) protein levels of Bax and Bcl-2 in cells determined by Western blot analysis (unpaired *t* test, **p* < 0.05). N = 10 in each group. Data were exhibited as mean ± SEM from three independent experiments. Representative images are provided.

scarring of glomerular mesangial cells are also the hallmark events during DN.[7] The MSC-Evs/exosomes have been seen as cell-free therapies in several human diseases including kidney injury.[25] A study by Grange et al showed that injection of labeled MSC-Evs leads to an accumulation of these Evs in the kidneys of a mouse model of acute kidney injury compared to the healthy controls.[26] More relevantly, MSC-derived exosomes have been validated as

one of the renal trophic factors as they may serve as a promising tool in DN prevention.[27] Likewise, MSC-derived exosomes have been found to improve renal function and the histological restoration of renal tissues in DN through inducing autophagy.[28] Clinically, a recent study noted the efficacy of MSC-exosomes in clinical use, where patients over 6 months of chronic kidney disease showed improved symptom, reduced serum creatinine, and improved urinary albumin creatinine ratio without side effects following MSC-exosome administration.[29]

Since the unique roles of exosomes in various biological functions are usually involving the transfer of biomolecules including RNA, proteins, enzymes, and lipids,[30] we next explored the potential molecules involved in protective events mediated by MSC-derived exosomes. miR-125a, which was abundantly found in the extracted exosomes as compared to the supernatant after centrifugation, was selected as the subject of the present study. This miRNA has been noted to be carried by MSC-exosomes and to promote endothelial cell angiogenesis.[8] Importantly, miR-125a has been demonstrated to regulate IL-6R expression in DN patients with a potential function in DN prevention.[18] Here, our study found that downregulation of miR-125a in the exosomes blocked the protective functions of the adMSC-exosomes in DN rat models and in HG-treated GMCs. These results indicated that miR-125a was, at least partially, responsible for the MSC-exosome-mediated kidney protection events.

Next, we identified HDAC1 as a target mRNA of miR-125a through online prediction and a dual luciferase reporter assay. Intriguingly, HDAC1 was found to interact with ET-1,[21] and both of them have been noted to be highly expressed in DN.[20,22] Then, we supposed that these factors are possibly involved in DN progression. High expression of HDAC1 and ET1 was found in DN rat models and in HG-induced GMCs, and then the interaction between HDAC1 and ET1 was validated in cells by an RNA-pull down assay. Excessive proliferation of glomerular mesangial cells and expansion of mesangium may occlude glomerular capillaries and persistently damages glomerular tissue integrity and renal function.[7] Importantly, our study found that artificial overexpression of HDAC1 increased the secretion of IL-6 in and promoted proliferation of HG-treated GMCs, but this promotion was inhibited by ET-1 silencing, indicating that HDAC1 could aggregate DN progression through up-regulating ET-1. The associations between ET-1 and diabetes and its complications have been largely concerned. For instance, ET1 has been reported to induce insulin resistance,[31] and therefore it is potentially relevant to the blood glucose level. High expression of ET-1 has also been suggested to increase the

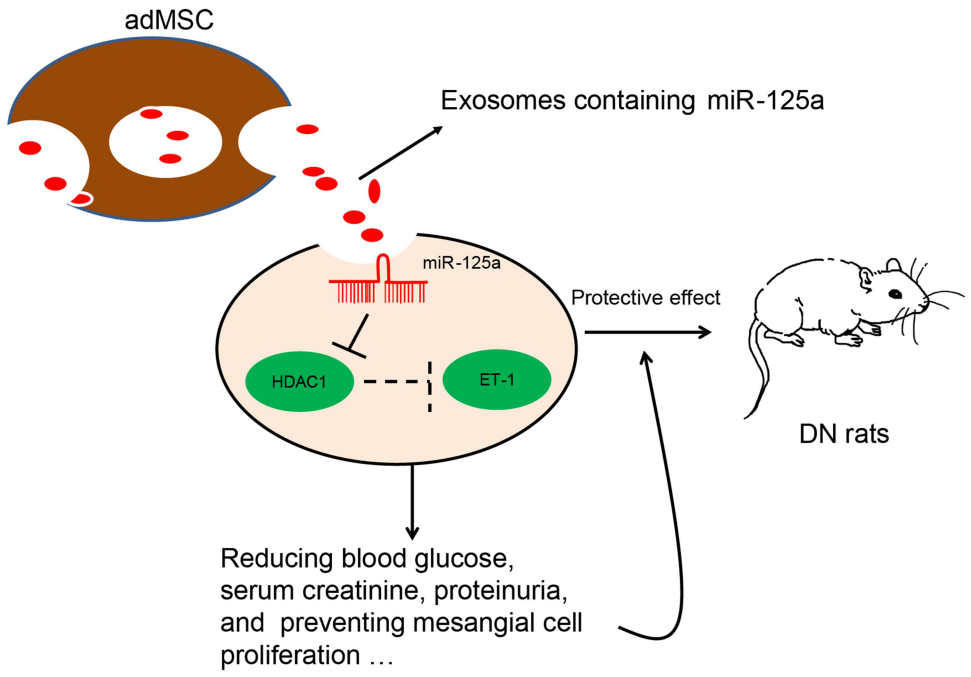

Figure 7 A diagram for molecular mechanism. adMSC-derived exosomes carry miR-125a to decrease the levels of blood glucose, serum creatinine and urinary protein in DN model rats. In HG-treated GMCs, exosomal miR-125a inhibits cell proliferation and expression of fibrosis-related factors to alleviate DN progression. miR-125a directly binds to HDAC1, which interacts with ET-1 to up-regulate ET-1 expression. Down-regulation of HDAC1 and ET-1 is involved in the miR-125a-mediated kidney protective events.

glomerular permeability,[32] which in turn leads to an increase in the level of serum creatinine. Moreover, upregulation of ET-1 was reported to be positively associated with the proteinuria level in patients with DN.[33] In concert with this, blockage in ET-1 was found to reduce proteinuria.[34] In addition, ET-1 has been found to promote proliferation of mesangial cells and ECM accumulation by binding to the Endothelin A receptor.[35] In addition, ET-1 has also shown pro-fibrotic and pro-inflammatory roles in diabetic complications.[36] Further experiments identified that the suppressive functions of Exo-mimic in either DN rats or in HG-treated GMCs were blocked upon HDAC1 upregulation. Collectively, these results evidenced that MSC-derived exosomes exerted kidney protective functions in DN through miR-125a and the following downregulation of HDAC1 and ET-1.

Conclusion

To sum up, the current study validated that adMSC-derived exosomes are promising tools to alleviate DN progression through carrying miR-125a. This miRNA could directly bind to HDAC1 and further down-regulate ET-1 expression to reduce DN-like symptoms and renal impairment (Figure 7). These findings may offer novel insights into DN prevention and treatment. However, the potential mechanical molecules involved in the DN development are too large to be clearly identified, we hope more studies will be launched in the future to provide new understandings and to develop potential therapeutic options for DN treatment.

Disclosure

The authors declare no conflicts of interest.

References

1. Umanath K, Lewis JB. Update on diabetic nephropathy: core curriculum 2018. *Am J Kidney Dis*. 2018;71(6):884–895. doi:10.1053/j.ajkd.2017.10.026
2. Flyvbjerg A. The role of the complement system in diabetic nephropathy. *Nat Rev Nephrol*. 2017;13(5):311–318. doi:10.1038/nrneph.2017.31
3. Geng XD, Wang WW, Feng Z, et al. Identification of key genes and pathways in diabetic nephropathy by bioinformatics analysis. *J Diabetes Investig*. 2019;10(4):972–984. doi:10.1111/jdi.12986
4. Jafari D, Malih S, Eslami SS, et al. The relationship between molecular content of mesenchymal stem cells derived exosomes and their potentials: opening the way for exosomes based therapeutics. *Biochimie*. 2019;165:76–89. doi:10.1016/j.biochi.2019.07.009
5. Cosenza S, Ruiz M, Maumus M, Jorgensen C, Noel D. Pathogenic or therapeutic extracellular vesicles in rheumatic diseases: role of mesenchymal stem cell-derived vesicles. *Int J Mol Sci*. 2017;18(4):889. doi:10.3390/ijms18040889
6. Yamashita T, Takahashi Y, Takakura Y. Possibility of exosome-based therapeutics and challenges in production of exosomes eligible for therapeutic application. *Biol Pharm Bull*. 2018;41(6):835–842. doi:10.1248/bpb.b18-00133
7. Tung CW, Hsu YC, Shih YH, Chang PJ, Lin CL. Glomerular mesangial cell and podocyte injuries in diabetic nephropathy. *Nephrology (Carlton)*. 2018;23 Suppl 4:32–37. doi:10.1111/nep.13451
8. Liang X, Zhang L, Wang S, Han Q, Zhao RC. Exosomes secreted by mesenchymal stem cells promote endothelial cell angiogenesis by transferring miR-125a. *J Cell Sci*. 2016;129(11):2182–2189. doi:10.1242/jcs.170373
9. Condrat CE, Thompson DC, Barbu MG, et al. miRNAs as biomarkers in disease: latest findings regarding their role in diagnosis and prognosis. *Cells*. 2020;9(2):276. doi:10.3390/cells9020276
10. Inoue K, Gan G, Ciarleglio M, et al. Podocyte histone deacetylase activity regulates murine and human glomerular diseases. *J Clin Invest*. 2019;129(3):1295–1313. doi:10.1172/JCI124030
11. Chen S, Tang Y, Liu Y, et al. Exosomes derived from miR-375-overexpressing human adipose mesenchymal stem cells promote bone regeneration. *Cell Prolif*. 2019;52(5):e12669. doi:10.1111/cpr.12669
12. Zhang J, Zhang X. Ischaemic preconditioning-induced serum exosomes protect against myocardial ischaemia/reperfusion injury in rats by activating the PI3K/AKT signalling pathway. *Cell Biochem Funct*. 2020.
13. Tong Y, Liu S, Gong R, Zhong L, Duan X, Zhu Y. Ethyl vanillin protects against kidney injury in diabetic nephropathy by inhibiting oxidative stress and apoptosis. *Oxid Med Cell Longev*. 2019;2019:2129350. doi:10.1155/2019/2129350
14. Xiang E, Han B, Zhang Q, et al. Human umbilical cord-derived mesenchymal stem cells prevent the progression of early diabetic nephropathy through inhibiting inflammation and fibrosis. *Stem Cell Res Ther*. 2020;11(1):336. doi:10.1186/s13287-020-01852-y
15. Li P, Bukhari SNA, Khan T, et al. Apigenin-loaded solid lipid nanoparticle attenuates diabetic nephropathy induced by streptozotocin nicotinamide through Nrf2/HO-1/NF-kB signalling pathway. *Int J Nanomedicine*. 2020;15:9115–9124. doi:10.2147/IJN.S256494
16. Wang S, Wen X, Han XR, et al. Repression of microRNA-382 inhibits glomerular mesangial cell proliferation and extracellular matrix accumulation via FoxO1 in mice with diabetic nephropathy. *Cell Prolif*. 2018;51(5):e12462. doi:10.1111/cpr.12462
17. Horii Y, Muraguchi A, Iwano M, et al. Involvement of IL-6 in mesangial proliferative glomerulonephritis. *J Immunol*. 1989;143(12):3949–3955.
18. Li C, Lei T. Rs12976445 polymorphism is associated with risk of diabetic nephropathy through modulating expression of microRNA-125 and interleukin-6R. *Med Sci Monit*. 2015;21:3490–3497. doi:10.12659/MSM.894987
19. Ma J, Zhao N, Du L, Wang Y. Downregulation of lncRNA NEAT1 inhibits mouse mesangial cell proliferation, fibrosis, and inflammation but promotes apoptosis in diabetic nephropathy. *Int J Clin Exp Pathol*. 2019;12(4):1174–1183.
20. Das F, Maity S, Ghosh-Choudhury N, Kasinath BS, Ghosh Choudhury G. Deacetylation of S6 kinase promotes high glucose-induced glomerular mesangial cell hypertrophy and matrix protein accumulation. *J Biol Chem*. 2019;294(24):9440–9460. doi:10.1074/jbc.RA118.007023
21. Rosano L, Cianfrocca R, Tocci P, et al. beta-arrestin-1 is a nuclear transcriptional regulator of endothelin-1-induced beta-catenin signaling. *Oncogene*. 2013;32(42):5066–5077. doi:10.1038/onc.2012.527
22. Lenoir O, Milon M, Virsolvy A, et al. Direct action of endothelin-1 on podocytes promotes diabetic glomerulosclerosis. *J Am Soc Nephrol*. 2014;25(5):1050–1062. doi:10.1681/ASN.2013020195
23. Kim Y, Park CW. New therapeutic agents in diabetic nephropathy. *Korean J Intern Med*. 2017;32(1):11–25. doi:10.3904/kjim.2016.174

24. Xue C, Mei CL. Polycystic kidney disease and renal fibrosis. *Adv Exp Med Biol*. 2019;1165:81–100.
25. Jafarinia M, Alsahebfosoul F, Salehi H, Eskandari N, Ganjalikhani-Hakemi M. Mesenchymal stem cell-derived extracellular vesicles: a novel cell-free therapy. *Immunol Invest*. 2020:1–23.
26. Grange C, Tapparo M, Bruno S, et al. Biodistribution of mesenchymal stem cell-derived extracellular vesicles in a model of acute kidney injury monitored by optical imaging. *Int J Mol Med*. 2014;33(5):1055–1063. doi:10.3892/ijmm.2014.1663
27. Nagaishi K, Mizue Y, Chikenji T, et al. Mesenchymal stem cell therapy ameliorates diabetic nephropathy via the paracrine effect of renal trophic factors including exosomes. *Sci Rep*. 2016;6(1):34842. doi:10.1038/srep34842
28. Ebrahim N, Ahmed IA, Hussien NI, et al. Mesenchymal stem cell-derived exosomes ameliorated diabetic nephropathy by autophagy induction through the mTOR signaling pathway. *Cells*. 2018;7(12):226. doi:10.3390/cells7120226
29. Mendt M, Rezvani K, Shpall E. Mesenchymal stem cell-derived exosomes for clinical use. *Bone Marrow Transplant*. 2019;54(Suppl 2):789–792. doi:10.1038/s41409-019-0616-z
30. Gurunathan S, Kang MH, Jeyaraj M, Qasim M, Kim JH. Review of the isolation, characterization, biological function, and multifarious therapeutic approaches of exosomes. *Cells*. 2019;8(4):307. doi:10.3390/cells8040307
31. Ahlborg G, Lindstrom J. Insulin sensitivity and big ET-1 conversion to ET-1 after ETA- or ETB-receptor blockade in humans. *J Appl Physiol*. 2002;93(6):2112–2121. doi:10.1152/japplphysiol.00477.2002
32. Kasztan M, Pollock DM. Impact of ET-1 and sex in glomerular hyperfiltration in humanized sickle cell mice. *Clin Sci (Lond)*. 2019;133(13):1475–1486. doi:10.1042/CS20190215
33. Zanatta CM, Veronese FV, Loreto Mda S, et al. Endothelin-1 and endothelin a receptor immunoreactivity is increased in patients with diabetic nephropathy. *Ren Fail*. 2012;34(3):308–315. doi:10.3109/0886022X.2011.647301
34. Fukui M, Nakamura T, Ebihara I, et al. Gene expression for endothelins and their receptors in glomeruli of diabetic rats. *J Lab Clin Med*. 1993;122(2):149–156.
35. Badr KF, Murray JJ, Breyer MD, Takahashi K, Inagami T, Harris RC. Mesangial cell, glomerular and renal vascular responses to endothelin in the rat kidney. Elucidation of signal transduction pathways. *J Clin Invest*. 1989;83(1):336–342. doi:10.1172/JCI113880
36. Ergul A. Endothelin-1 and diabetic complications: focus on the vasculature. *Pharmacol Res*. 2011;63(6):477–482. doi:10.1016/j.phrs.2011.01.012